

# TEMPERATURE DRIVEN TUNING OF THE STRUCTURE AND MAGNETIC PROPERTIES OF OXIDES OF ERBIUM AND CHROMIUM AT NANOSCALE

Oimang Borang<sup>1</sup>, S. Srinath<sup>2</sup>, S. N. Kaul<sup>3</sup>, Y. Sundarayya<sup>4</sup>

<sup>1</sup>Department of Physics, Nagaland University, Lumami -798627, Nagaland, India

<sup>2</sup>School of Physics, University of Hyderabad, Prof. C.R. Rao Road, Gachibowli, Hyderabad – 500046, India

<sup>3</sup>School of Physics, University of Hyderabad, Prof. C.R. Rao Road, Gachibowli, Hyderabad – 500046, India

<sup>4</sup>Department of Physics, Nagaland University, Lumami -798627, Nagaland, India & <sup>2</sup>School of Physics, University of Hyderabad, Prof. C.R. Rao Road, Gachibowli, Hyderabad – 500046, India

## Abstract

We report the synthesis of homogeneous single phase nanoparticles of  $\text{ErCrO}_4$  and  $\text{ErCrO}_3$  by a modified sol-gel hydrothermal method. Temperature dependent annealing results in the formation of  $\text{ErCrO}_4$  and  $\text{ErCrO}_3$  phases at low and high temperatures. Analysis of the X-ray diffractograms reveal that  $\text{ErCrO}_4$  crystallizes into tetragonal structure with space group  $I41/amd$  and  $\text{ErCrO}_3$  into orthorhombic structure with space group  $Pnma$ . Morphological analysis confirms uniformly distributed nanoparticles of  $\text{ErCrO}_4$  with size 20 nm and  $\text{ErCrO}_3$  with 70 nm. DC magnetic measurements show that  $\text{ErCrO}_4$  undergoes a paramagnetic-antiferromagnetic transition at 16 K, the Néel temperature ( $T_N$ ) due to the superexchange  $\text{Er-O-Cr-O-Er}$  antiferromagnetic interactions and that the  $\text{Er}^{3+}$  ions alone carry a magnetic moment while Cr exists in  $\text{Cr}^{3+}$  ( $3d^0$ ) valence state. And  $\text{ErCrO}_3$  undergoes paramagnetic-antiferromagnetic transition at 137 K ( $T_N$ ), due to  $\text{Cr-O-Cr}$  superexchange interaction, with canting of spins at Cr sites below Néel temperature, attributed to antisymmetric Dzyaloshinsky-Moriya (DM) exchange interaction between neighbouring spins.

**Keywords:** Sol-gel processing, Nanocrystalline materials, Antiferromagnetics

**PACS:** 81.20.Fw, 73.63.Bd, 75.50.Ee

\*\*\*

## 1. INTRODUCTION

At recent, the global development is based upon the technologies corresponding to the useful material properties obtained as an outcome of the research work in the field of materials. Multiferroic and/or magneto-electric field is one among those research areas, where a material exhibits multiform effects in a single phase material [1–3]. The combination of rare earth and transition metal ions has manifested as one of the most relevant group of compounds for investigations of manifold magnetic interactions in magnetolectric/multiferroic compound due to their mechanical, dielectric, optical and magnetic properties which make them suitable material to study. Since transition metal are tending to have variable oxidation states, they prone to form oxides with R in different combinations. The present paper focuses on one of those exotic combinations of rare-earth with transition metal, in particular erbium and chromium that form  $\text{ErCrO}_3$  and  $\text{ErCrO}_4$ , obtained from hydrothermal synthesis.

$\text{ErCrO}_3$ , one of the orthochromite in  $\text{RCrO}_3$ , exhibits complex magnetic behavior due to the magnetic exchange interactions among  $\text{Cr}^{3+}$  -  $\text{Cr}^{3+}$ ,  $\text{Cr}^{3+}$  -  $\text{Er}^{3+}$  and  $\text{Er}^{3+}$  -  $\text{Er}^{3+}$  mediated by oxygen. Among these interactions,  $\text{Cr}^{3+}$  -  $\text{Cr}^{3+}$  is the strongest that is responsible to an antiferromagnetic ordering but with

canting of the spins of the Cr sublattices at the Néel temperature,  $T_N$  (~ 137 K), leads to weak ferromagnetism [4]. Among the others, the presence of  $\text{Er}^{3+}$  -  $\text{Er}^{3+}$  interaction may be observed at very low temperatures (~ 10 K) and the  $\text{Er}^{3+}$  -  $\text{Cr}^{3+}$  interaction is accountable to the phenomena like spin reorientation and magnetization reversal below a compensation temperature [5–7].  $\text{ErCrO}_4$  belongs to a family of  $\text{RCrO}_4$  compounds where the Chromium is stabilized in an unusual oxidation state of +5 [8, 9]. The magnetic structure of  $\text{RCrO}_4$  with R = Nd–Yb is described as ferromagnetic, while  $\text{RCrO}_4$  oxides with R = Sm, Eu and Lu are shown to be antiferromagnetic [10, 11]. The widely different magnetic behaviour of  $\text{ErCrO}_4$  could be due to the changes in the pathways of Er-O-Cr superexchange interactions with Néel temperatures ~ 20 K.

Temperature driven synthesis of single phase  $\text{ErCrO}_3$  and  $\text{ErCrO}_4$  compound by modified sol-gel hydrothermal process has captivated our attention due to their intriguing crystal structures and magnetic properties obtained as a result of Cr valence. While the former crystallize into orthorhombic structure with space group  $Pbnm$ , the later forms tetragonal structure with space group  $I41/amd$ .  $\text{ErCrO}_3$  and  $\text{ErCrO}_4$  are highly attractive because of their large coupling strength due to their fourfold anisotropic term and hence play an

important role in determining the different magnetic phases in orthochromites due to spin reorientation transitions. This special nature of orthochromites made it interesting to study the magnetic phases depending on temperature, pressure and applied magnetic field.

## 2. EXPERIMENTAL SECTION

The  $\text{ErCrO}_3$  and  $\text{ErCrO}_4$  samples were prepared from appropriate hydrated salts of rare earth nitrites and chromium nitrates using sol gel by hydrothermal method [12]. To proceed the synthesis the stoichiometric amount of the rare earth nitrites (Alfa-aesar 99.9%), chromium nitrate hydrate (Alfa-aesar 99.9%) and citric acid were taken in 1:1:1 ratio. In our deliberated sample, the powder of the oxides was dissolved thoroughly in deionized water to conglomerate the metal and citrate ions. The solution was followed by the drop wise addition of ammonia to raise the PH value up to a basic level of 9-10. The solution was allowed for calcinations in a hydrothermal bomb at 473 K followed by centrifugation after the temperature falls at room degree in order to separate the phase. After disposing the waste water the sol has been heated at around 70-80 C to let it dry. The dried sample was crushed and makes a pellet which has been heated again at 973 K to get a crystal form structure of  $\text{ErCrO}_3$  nanoparticles and at 773 K to get the  $\text{ErCrO}_4$  nanoparticles. Further, the synthesized sample were characterized by X-ray powder diffraction using Bruker D8 Advance diffractometer with  $\text{Cu-K}\alpha$  radiation ( $\lambda = 1.54056 \text{ \AA}$ ) within the range  $10\text{-}90^\circ$ . The morphology of the samples was studied by means of field-emission scanning electron microscopy (Carl Zeiss ULTRA-55 FESEM). Magnetic measurements were carried out with a vibrating sample magnetometer in a Physical Property Measurement System (PPMS).

## 3. RESULTS AND DISCUSSIONS

XRD pattern of the synthesized-sample is found to be amorphous. Figure 1(a) and 1(b) show the Rietveld profile matching of the X-ray diffractograms of  $\text{ErCrO}_4$  and  $\text{ErCrO}_3$  obtained after annealing the as synthesized sample at 773 K and 993 K respectively for 12 hr in air. It was found from the analysis that  $\text{ErCrO}_4$  crystallizes into tetragonal structure with space group  $I41/amd$  with lattice parameters  $a = b = 7.0937 \text{ \AA}$  and  $c = 6.2408 \text{ \AA}$ . The inset of figure 1(a) shows the unit cell structure of  $\text{ErCrO}_4$ , obtained from X-ray data analysis. The average crystallite size of  $\text{ErCrO}_4$  nanoparticles obtained from the Scherer's formula is 21 (1) nm [13]. And  $\text{ErCrO}_3$  crystallizes into orthorhombic structure with space group  $Pnma$  with lattice parameters  $a=5.5211 \text{ \AA}$ ,  $b=7.5290 \text{ \AA}$ ,  $c=5.2301 \text{ \AA}$ . The inset of figure 1(b) shows the unit cell structure of  $\text{ErCrO}_3$ , obtained from X-ray data analysis. The average crystallite size obtained for  $\text{ErCrO}_3$  is 35 (1) nm. Figures 2(a) and 2(b) show the morphology of the  $\text{ErCrO}_4$  and  $\text{ErCrO}_3$  nanoparticles. The morphological analysis reveals that  $\text{ErCrO}_4$  nanoparticles are monodispersed with  $\sim 20 \text{ nm}$  size and  $\text{ErCrO}_3$  nanoparticles with  $\sim 70 \text{ nm}$ .

Figure 3 shows the field-cooled (FC) magnetization measurements on  $\text{ErCrO}_4$  and  $\text{ErCrO}_3$  nanoparticles in the

presence of an external magnetic field of 100 Oe in the temperature range  $2 \text{ K} \leq T \leq 250 \text{ K}$ . It shows the  $\text{ErCrO}_3$  undergoes a paramagnetic to antiferromagnetic transition at  $\sim 133 \text{ K}$ , the Néel temperature ( $T_N$ ) of the  $\text{Cr}^{3+}$  sublattice. The observed  $T_N$  of the  $\text{ErCrO}_3$  nanoparticles matches with the  $T_N$  (133 K) of the bulk sample reported elsewhere [7], confirms the Néel temperature does not get effected by the size of the  $\text{ErCrO}_3$  nanoparticles in discussion. On the other hand the field-cooled (FC) magnetization of  $\text{ErCrO}_4$  reveals that the sample undergoes a paramagnetic to antiferromagnetic transition at 16 K, which marks the Néel temperature ( $T_N$ ), below which the  $\text{Er}^{3+}$  moments order into an antiferromagnetic state. The  $T_N$  observed for nanocrystalline  $\text{ErCrO}_4$  is lower by  $\sim 5 \text{ K}$  compared to that reported for the bulk [9]. The reduced  $T_N$  is attributed to finite size effects.

Figures 4(a) and 4(b) shows the inverse susceptibility of  $\text{ErCrO}_4$  and  $\text{ErCrO}_3$  in the paramagnetic region in the temperature range 140 – 290 K. It is found that both the compounds follow a typical Curie-Weiss (CW) behavior. By fitting the CW law to  $\chi^{-1}(T)$ , we obtain the characteristic temperature for  $\text{ErCrO}_4$  and  $\text{ErCrO}_3$  to be  $\theta = -11.0(2) \text{ K}$  and  $-14.9(8) \text{ K}$  respectively. This confirms the presence of antiferromagnetic spin correlations in the compounds. The effective magnetic moment ( $\mu_{\text{eff}}$ ), deduced from the Curie constant, for  $\text{ErCrO}_4$  is  $9.959 \mu_B$ ; a value that is close to  $\mu_{\text{eff}}$  of  $\text{Er}^{3+}$  ( $9.4 \mu_B$ ). This implies that the magnetic moment on  $\text{Er}^{3+}$  completely accounts for the observed moment. It immediately follows that chromium exists in  $\text{Cr}^{5+}$  valance state and is non-magnetic ( $3d^0$ ). The effective magnetic moment obtained for  $\text{ErCrO}_3$  is  $8.823 \mu_B$ .

## 4. CONCLUSION

Monodisperse single phase  $\text{ErCrO}_4$  and  $\text{ErCrO}_3$  nanoparticles with an average crystallite size of 21 (1) nm and 35 (1) nm have been synthesized by a modified hydrothermal synthesis followed by annealing. Morphological studies show that the particles have uniform size distribution. DC magnetic measurements reveal that  $\text{ErCrO}_4$  undergoes a paramagnetic-antiferromagnetic transition at 16 K and that the  $\text{Er}^{3+}$  ions alone carry a magnetic moment while Cr exists in  $\text{Cr}^{5+}$  ( $3d^0$ ) valance state. On the other hand,  $\text{ErCrO}_3$  undergoes a paramagnetic-canted antiferromagnetic transition at 133 K, due to the presence of  $\text{Cr}^{3+} - \text{O} - \text{Cr}^{3+}$  exchange interactions driven by Dzyaloshinskii – Moriya interactions.

## ACKNOWLEDGMENT

Authors are thankful to the School of Engineering and Technology (SEST) for the X-ray diffractograms, School of Physics for FESEM images, Centre for Nanotechnology, University of Hyderabad (UoH) for magnetic measurements. ON wishes to thank UGC for the financial assistance in the form of National Fellowship for Higher Education (NFHE) of ST students.

REFERENCES

- [1] I.E. Dzyaloshinskii, Soviet Physics, **10**, 628 (1960).
- [2] D.N. Astrov, Soviet Physics, **11**, 708 (1960).
- [3] G.T. Rado and V.J. Folen, Phys. Rev. Lett., **7**, 310 (1961).
- [4] T.Yamaguchi, *J.Phys.Chem. Solids***35**, 479 (1974).
- [5] T. Sakata, and A. Enomura,*Phys. Status Solidi A***52**, 311 (1979).
- [6] K.B. Aring, and A. J. Sievers,*J. Appl. Phys.***41**, 1197 (1970).
- [7] B. Rajeswaran,D. I. Khomskii,A. K. Zvezdin,C. N. R. Raoand A. Sundaresan,*Phys.Rev.B***86**, 214409 (2012).
- [8] E. Jiménez, J. Isasi, M.T. Fernández, R. Sáez-Puche, *J. Alloys Comp.***344**, 369–374 (2002).
- [9] R. S. Puche, E. Climent, M. G. Rabie, J. Romero, and J. M. Gallardo, *J. Phys.:Conf. Series***325**, 012012 (2011).
- [10] H.Walter, H.G. Kahle, K. Mulder, H.C. Schopper, H. Schwarz, *Int. J. Magn.***5**, 129 (1973).
- [11] E. Jiménez, J. Isasi, R. S. Puche, *J. Alloys Comp.***312**, 53 (2000).
- [12] AdhishJaiswal, Raja Das, K. Vivekanand, TuhinMaity, Priya Mary Abraham, SugunaAdyanthaya, and Pankaj Poddar, *J. Appl. Phys.* **107**, 013912 (2010).
- [13] B.D. Cullity, Elements of X-ray diffraction, Addison-Wiley, Massachusetts (1978).

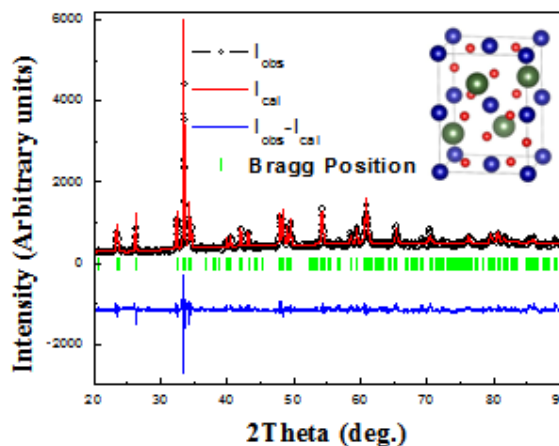


Fig 1(b) Powder X-Ray diffractogram of ErCrO<sub>3</sub>

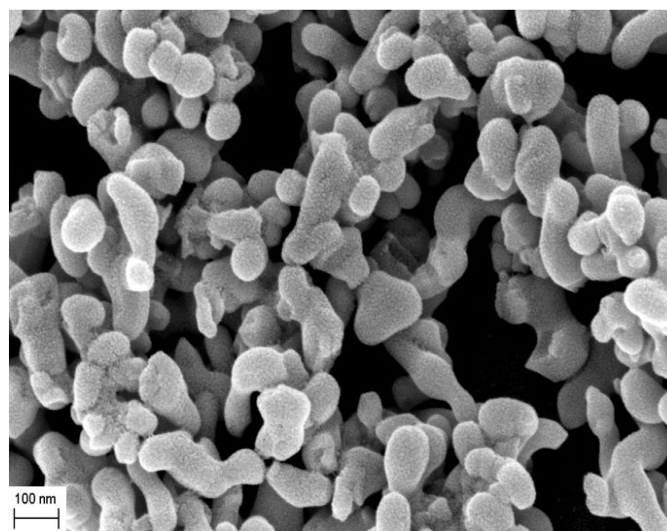
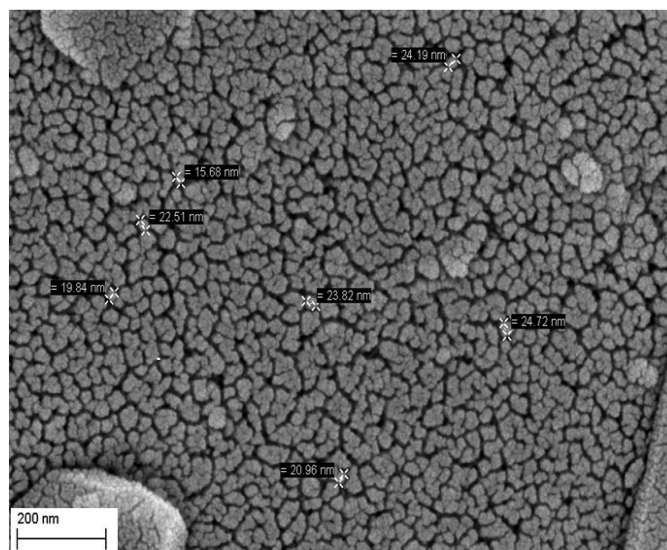


FIGURE CAPTIONS

Fig.1(a). Rietveld profile matching of ErCrO<sub>4</sub>. The inset shows the unit cells structures of ErCrO<sub>4</sub>.  
 Fig. 1(b). Rietveld profile matching of ErCrO<sub>3</sub>. The inst shows the unit cells structureofErCrO<sub>3</sub>.  
 Fig. 2(a). Morophology of ErCrO<sub>4</sub> nanoparticles by FESEM.  
 Fig. 2(b). Morphology of ErCrO<sub>3</sub> nanoparticles by FESEM.  
 Fig.3. FC magnetization of ErCrO<sub>4</sub> and ErCrO<sub>3</sub> nanoparticles.  
 Fig. 4. C-W analysis of 1/χ vs T of ErCrO<sub>4</sub>(a) and ErCrO<sub>3</sub> (b).

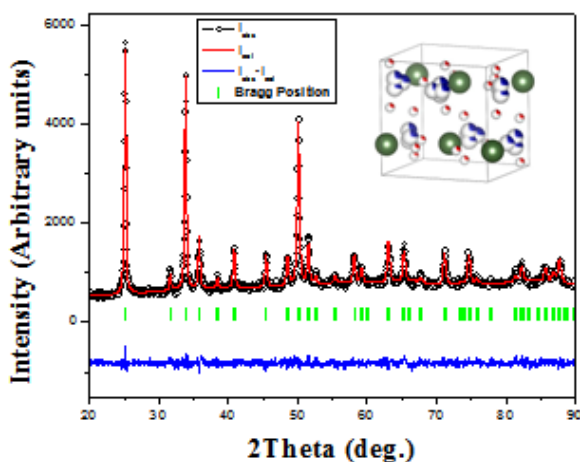


Fig 1 (a) Powder X-Ray diffractogram of ErCrO<sub>4</sub>

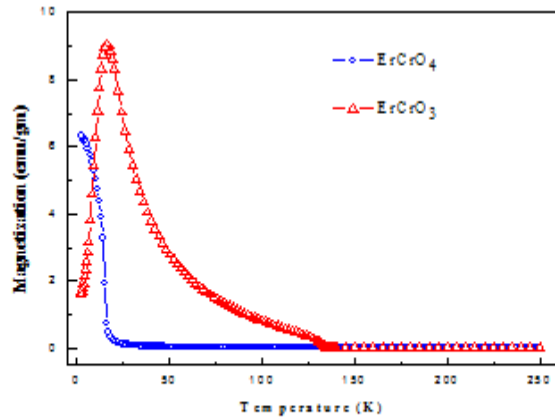


Fig.3 FC magnetization of  $\text{ErCrO}_4$  and  $\text{ErCrO}_3$  nanoparticles

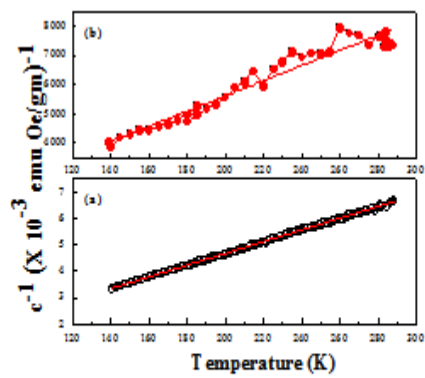


Fig. 4 C-W analysis of  $1/\chi$  vs T of  $\text{ErCrO}_4$ (a) and  $\text{ErCrO}_3$  (b)